Genes to Cells

Evidence for a role of angiopoietin-like 7 (ANGPTL7) in extracellular matrix formation of the human trabecular meshwork: implications for glaucoma

Núria Comes, LaKisha K. Buie and Teresa Borrás*

Department of Ophthalmology, University of North Carolina School of Medicine, Chapel Hill, NC, USA

The trabecular meshwork tissue controls the drainage of the aqueous humor of the eye. A dysfunctional trabecular meshwork leads to an altered fluid resistance, which results in increased intraocular pressure (IOP). IOP is the major risk factor of glaucoma, the second-leading cause of blindness in the developed world. In the search for genes altered by glaucomatous insults, we identified angiopoietin-like7 (ANGPTL7), a member of the ANGPTL family. Although structurally related to the angiopoietins, ANGPTL7's function is poorly understood. Because ANGPTL7 is secreted and because extracellular matrix (ECM) deposition and organization is critical for aqueous humor resistance, we investigated the effect of ANGPTL7 on relevant trabecular meshwork ECM genes and proteins. We find that overexpression of ANGPTL7 in primary human trabecular meshwork cells altered the expression of *fibronectin, collagens type I, IV & V, myocilin, versican, and MMP1*. ANGPTL7 also interfered with the fibrillar assembly of fibronectin. Finally, we find that silencing ANGPTL7 during the glucocorticoid insult significantly affected the expression of other steroid-responsive proteins. These results indicate that ANGPTL7 modulates the trabecular meshwork's ECM as well as the response of this tissue to steroids. Together with previous findings, these properties strengthen ANGPTL7's candidacy for the regulation of IOP and glaucoma.

Introduction

Angiopoietin-like (ANGPTL) molecules comprise a family of proteins that are structurally related to the angiogenic factors angiopoietins (Oike & Tabata 2009). As angiopoietins, these proteins contain an N-terminal coiled-coil domain and a C-terminal fibrinogen-like domain. However, the ANGPTLs are unable to bind the angiopoietin receptors Tie2 or Tie1 (Kim *et al.* 2000; Camenisch *et al.* 2002; Katoh & Katoh 2006) implying that they would not regulate blood vessel formation via the same mechanism as the angiopoietins. There are seven members of ANGPTLs (from 1 to 7) (Katoh & Katoh 2006). Although some members of the ANGPTLs (1, 2, 3, 4 and 6) have been shown to be potent regulators of angiogenesis (Oike *et al.* 2004; Hato *et al.* 2008), they appear to also exhibit unrelated functions such as induction of inflammation and regulation of lipid and glucose metabolism (Ono *et al.* 2003; Oike *et al.* 2005; Xu *et al.* 2005). ANGPTLs are secreted glycoproteins. They are found in the culture medium of ANGPTL transfected cells (Kim *et al.* 1999; Oike *et al.* 2004) (this study), and some of them, in the circulatory system of living rats and humans (Oike *et al.* 2004, 2005).

Angiopoietin-like 7 is the least studied of all family members. It is a secreted 45-kDa glycoprotein that folds into a homotetramer structure linked by disulfide bonds. ANGPTL7 was originally discovered in the stromal layer of the cornea and termed *cornea-derived transcript 6* (CDT6) (Peek *et al.* 1998). In the cornea, ANGPTL7/CDT6 was speculated to function as a negative regulator of angiogenesis and to possibly contribute to the avascular nature of this tissue (Peek *et al.* 2002). Human melanoma cells stably transfected with ANGPTL7/CDT6 induced changes in some extracellular matrix (ECM) components *in vitro* and led to the reduction of tumor growth in a mouse xenograph model compared to controls (Peek *et al.*

Communicated by: Moshe Yaniv
**Correspondence*: tborras@med.unc.edu

DOI: 10.1111/j.1365-2443.2010.01483.x

2002). However, subsequent reports using immunocompetent mice showed that ANGPTL7/CDT6 had no effect on tumor growth (Bouis *et al.* 2003, 2007), making controversial the angiogenic properties of this gene.

Our laboratory first reported that ANGPTL7/CDT6 was moderately expressed in the human trabecular meshwork (Gonzalez *et al.* 2000). Sequences of one thousand clones from the cDNA library of a perfused postmortem human pair of eyes from a single individual contained two clones of ANGPTL7/CDT6 (Gonzalez *et al.* 2000). Following studies showed that the ANGPTL7/CDT6 gene was specifically upregulated by dexamethasone (DEX) in primary human trabecular meshwork cells (HTM), the eye tissue associated with regulation of aqueous humor outflow facility (Lo *et al.* 2003). In fact, we showed that ANGPTL7/CDT6 was among the top twenty most upregulated genes when comparing HTM steroid-treated cells to those originating from the optic nerve head, also treated with DEX (Lo *et al.* 2003). Our original results have since then been confirmed and validated by several other laboratories. Sequences of ~3000 clones from nonperfused, pooled human trabecular meshworks detected 15 ANGPTL7/CDT6 clones (Tomarev *et al.* 2003a), placing the gene among the 15 most abundant in such cDNA library. In a different study, microarrays analysis of DEX-treated primary HTM cells showed ANGPTL7/CDT6 as the second most upregulated gene when compared to untreated cells (Rozsa *et al.* 2006).

The trabecular meshwork, localized at the angle formed by the cornea and the iris, is the main route for the outflow of the aqueous humor of the eye (Bill & Mäepea 1994). This tissue, which includes trabecular meshwork cells and cells of the Schlemm's canal, is avascular and is responsible for the maintenance of intraocular pressure (IOP). The trabecular meshwork cells are embedded in a loose ECM, which forms a spongiform-like unique architecture. All components of the outflow tissue, in particular the composition and quality of the ECM, play an important role in establishing the resistance required to attain physiologic pressure. Dysfunction of the trabecular meshwork leads to an increase in resistance to the eye fluid and to elevated IOP. Increased IOP creates a mechanical stress situation which, in a not well-understood manner, is transmitted to the back of the eye and exerts damage to the retinal ganglion cells (RGC) and to their axons (optic nerve). Death of RGCs impedes transmission of the visual signal to the brain and results in progressive loss of visual field and irreversible blindness. The resulting disease is glaucoma, the second leading cause of blindness worldwide (Quigley 1996). Elevated IOP is the major risk factor for glaucoma and lowering IOP is currently the only available treatment for all types of glaucoma.

Interestingly, the ANGPTL7/CDT6 gene maps to the long arm of chromosome 1 (1p36.22), within the chromosomal locus of the GLC3B region, that has been associated with a recessive form of congenital glaucoma (Akarsu *et al.* 1996). ANGPTL7/CDT6 is located within an intron of the MTOR gene, a serine-threonine kinase involved in cellular responses to stress (http://smd.stanford.edu/cgi-bin/source/sourceSearch). Furthermore, its regulation of expression in the trabecular meshwork has been associated with several glaucomatous conditions. In addition of being highly induced by glucocorticoids (Lo *et al.* 2003; Rozsa *et al.* 2006), which are responsible for steroid glaucoma (Armaly & Becker 1965; Tripathi *et al.* 1999), ANGPTL7/CDT6 was reported to be the second most upregulated gene by TGFβ2 (Zhao *et al.* 2004), a growth factor long known to be elevated in the aqueous humor of glaucoma patients (Tripathi *et al.* 1994). A proteomic analysis comparing trabecular meshworks from normal and glaucomatous patients showed ANGPTL7/CDT6 presence only in the diseased tissue (Bhattacharya *et al.* 2005). A subsequent study analyzing the relevance of ANGPTL7/CDT6 in glaucoma has been published (Kuchtey *et al.* 2008). The authors confirmed the DEX and TGFβ2 induction of ANGPTL7/CDT6 mRNA at the protein level, and showed a correlation between levels of ANGPTL7/CDT6 protein in the aqueous humor and glaucoma. An increase in collagen type I was also observed in an ANGPTL7/CDT6 stably transformed HTM cell line. Finally, a recent report from our laboratory using perfused human anterior segments, microarrays and real-time Taqman PCR has shown that expression of ANGPTL7/CDT6 is strongly upregulated by elevated IOP in the perfused human trabecular meshwork (Comes & Borrás 2009).

Because of the high relevance of the trabecular meshwork's ECM in the development of glaucoma, and of the association of overexpression of ANGPTL7/CDT6 with glaucomatous conditions, in this report we conducted a comprehensive study of the effect of ANGPTL7/CDT6 in matrix production of the trabecular meshwork cells. We found that elevated levels of ANGPTL7/CDT6 directly influence relevant ECM components and that its silencing during DEX treatment alters expression of DEX-regulated ECM

genes. ANGPTL7/CDT6 also affects protein levels of fibronectin and its distribution in the ECM of the primary human trabecular meshwork cells. We propose that this member of the angiopoietin family has a role in the organization of the ECM and that it functions as a mediator of DEX-induced matrix deposition in the human trabecular meshwork cells.

Results

Characterization of the ANGPTL7/CDT6 expression vector pNC1

The cDNA of the pNC1 expression vector was fully sequenced in both orientations and found to contain no mutations when compared to GenBank access number NM_021146. A cesium chloride–purified preparation was nucleofector-transfected into two different primary HTM cell lines (HTM-55 and HTM-69). At 72-h post-transfection, both cells and media were harvested for RNA and protein, respectively. Normalized real-time *Taq*Man PCR of the transfected versus mock-transfected samples showed an increased expression of ANGPTL7/CDT6 of 761-fold (636/909 range; $n = 3$; $P = 1.0 \times 10^{-7}$) and 312-fold (244/398 range; $n = 3$; $P = 9 \times 10^{-5}$) in HTM-55 and HTM-69, respectively (Fig. 1A). The transfection was repeated in each of the cell lines with similar results. Equivalent volumes of concentrated media from transfected and mock-transfected cells were analyzed by Western blots. A major protein band ~45 kDa ANGPTL7/CDT6 was detected in the media of cells transfected with pNC1, whereas it was not detected in the mock-transfected sample (Fig. 1B). This band corresponds to the glycosylated form of the ANGPTL7/CDT6 protein and it is larger than the 38 kDa expected by direct translation of its cDNA sequence (Peek *et al.* 2002).

Modulation of trabecular meshwork ECM genes' expression by ANGPTL7/CDT6

To determine the effect of ANGPTL7/CDT6 levels on the expression of ECM relevant proteins, we either overexpressed or silenced the gene and used 18S-normalized real-time *Taq*Man PCR to monitor expression of selected ECM genes. Nucleofector transfection of 2 μg of pNC1 in HTM-55 primary cells giving a 2188-fold (1989/2404 range; $P = 0.0001$) overexpression of ANGPTL7/CDT6 resulted in decrease of fibronectin (−3.2-fold, −3.0/−3.6 range; $P = 0.000004$), collagen type IA1 (−4.8-fold, −4.4/−5.0 range; $P = 0.00001$), collagen type IVA1 (−1.2-fold, −1.1/−1.4 range; $P = 0.0002$), collagen type VA1 (−2.0-fold, −1.7/−2.4 range; $P = 0.00001$), myocilin (−1.5-fold, 1.2/−2.6 range; $P = 0.0002$) and versican (−2.1-fold, −1.8/−2.5 range; $P = 0.0000004$). MMP1 levels were increased (1.9-fold, 1.3/2.5 range; $P = 0.0002$) (Fig. 2A) ($n = 3$). In another experiment where the ANGPTL7/CDT6 overexpression values reached 25,832-fold, induced changes on the expression of ECM proteins were all significant and in the same direction, with similar or more pronounced fold values.

Silencing of ANGPTL7/CDT6 by nucleofector transfection of 2 μg of siRNA in the same cell line reversed the effect. Compared to transfected scrambled siRNA, ANGPTL7/CDT6 levels were reduced −1.54-fold (−2.5/+1.1 range; $n = 3$; $P = 0.00004$), which corresponds to 35% silencing. This silencing extent lowered the levels of MMP1 (−1.3-fold, 1.4/−2.4 range; $P = 0.01$) and had minimal to no effect on collagen type IVA1 (−1.1-fold, −1.0/−1.1 range; $P = 0.11$) and collagen type IA1 (+1.1-fold, −1.0/+1.2 range; $P = 0.25$). Further, it increased the levels of fibronectin (1.9-fold, 1.6/2.4 range; $P = 0.03$), collagen type VA1 (1.6-fold, 1.4/1.8 range; $P = 0.002$), myocilin (2.0-fold, 1.8/2.3 range; $P = 0.00004$) and versican (1.5-fold, 1.3/1.7 range; $P = 0.03$) (Fig. 2B) ($n = 3$).

When overexpression and silencing were carried out in HTM-69 (originated from a different individual), the effect was very similar. At ANGPTL7/CDT6 overexpression levels of 786-fold (+744/+830 range), the transcription levels of six of the seven ECM proteins were lowered ($n = 3$). Fibronectin expression decreased −2.3-fold (−1.9/−2.7 range); collagen type IA1, −1.9-fold (−1.6/−2.3 range); collagen type IVA1, −1.2-fold (+1.1/−1.5 range); collagen type VA1, −1.7-fold (−1.4/−2.0 range), myocilin, −1.4-fold (−1.2/−1.8 range), and versican, −4.5-fold (−3.7/−5.3 range). MMP1 expression did not change. At levels of ANGPTL7/CDT6 silencing of 57% (−2.3 fold), the normalized expression levels were 1.4-fold (1.1/1.8 range) for fibronectin; 1.5-fold (1.4/1.5 range) for collagen type IA1; 2.3-fold (2.1/2.5 range) for collagen type IVA1; 4.8-fold (3.9/6.1 range) for collagen type VA1; 2.5-fold (2.2/2.9 range) for myocilin; 1.5-fold (1.4/+1.5) for versican and 1.4-fold (1.3/1.5 range) for MMP1.

The effect of overexpressing ANGPTL7/CDT6 on the ECM was also seen at the protein level. The media of cells transfected with pNC1 at 72-h

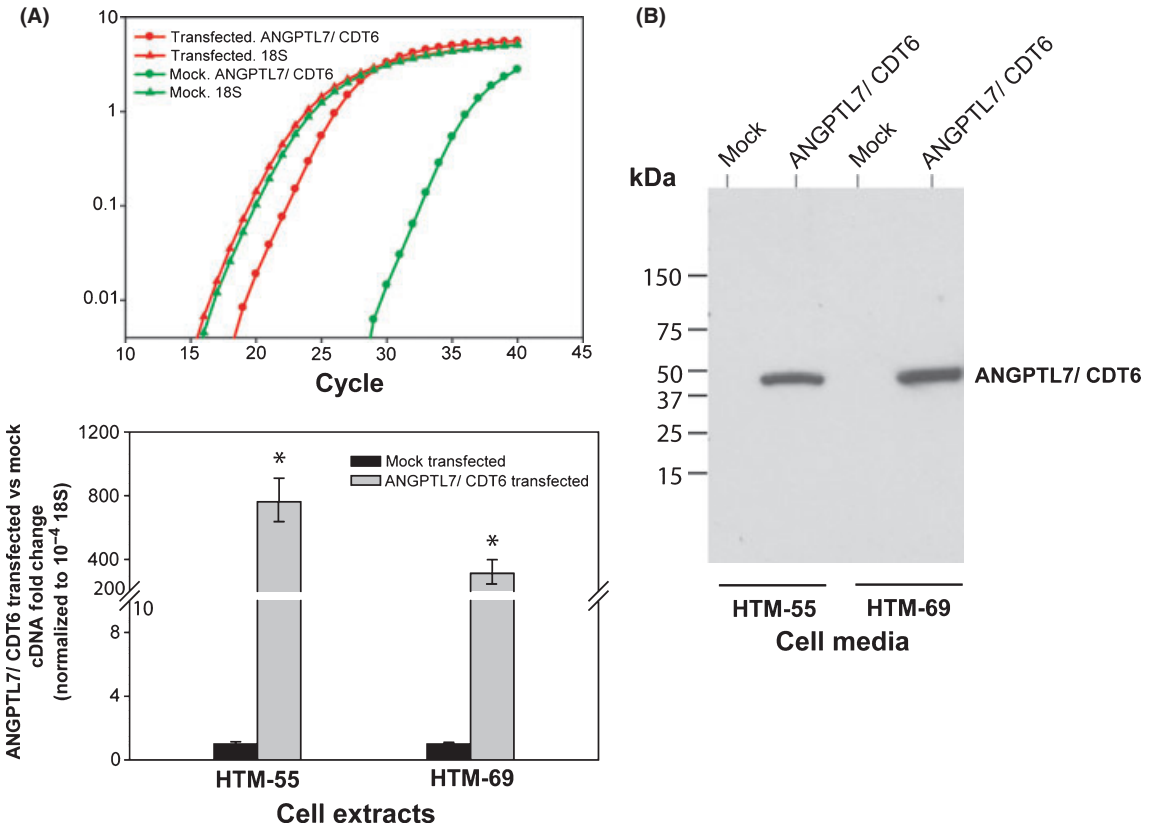

Figure 1 Analysis of the recombinant ANGPTL7/CDT6 plasmid (pNC1) in primary human trabecular meshwork cells. Two primary HTM cell lines (HTM-55 and HTM-69) were nucleofector-transfected with either ANGPTL7/CDT6 plasmid DNA or mock-transfected, and assayed at 72-h post-transfection. (A) Normalized ANGPTL7/CDT6 cDNA in the treated cells versus the mock-transfected cells. *Top panel*: representative C_T logarithmic curve of the hybridizations of ANGPTL7/CDT6 and endogenous 18S cDNAs from treated and mock-transfected cells with their corresponding *Taq*Man probes. *Bottom panel*: fold change of ANGPTL7/CDT6 cDNA in treated versus mock-transfected, normalized to 18S and expressed as fold change mean ± range ($n = 3$ $^{\star}P < 0.0001$). Upon normalization, the mock-transfected sample is given a value of 1. (B) ANGPTL7/CDT6 secreted protein detection by Western blot analysis. Equivalent volumes of cultured media from cells either mock or transfected with ANGPTL7/CDT6 were run in 4–15% polyacrylamide gels, transferred to PVDF membranes and incubated with ANGPTL7/CDT6 antibody ($n = 4$). Transfection of the pNC1 recombinant results in the overexpression of ANGPTL7/CDT6 mRNA and secreted protein.

post-transfection was analyzed for secreted fibronectin using an ELISA kit. In a representative experiment, we found that the levels of normalized fibronectin in the media of HTM-55 were 32.8% of the mock-transfected cells ($n = 3$; $P = 1 \times 10^{-6}$). Those in HTM-69 were 22.9% ($n = 3$; $P = 2 \times 10^{-5}$) (Fig. 3). Experiments were repeated in each of the cell lines with similar results.

We further assessed the structure of fibronectin fibrils in the extracellular matrix. We allowed cultured cells to deposit an ECM for 4.5 days and stained for fibronectin under nonpermeabilized conditions. In HTM control cells transfected with vehicle, fibronectin appeared as cross-linked fibrils showing the classical pattern of fibrils attached to the extracellular surface of cells and reaching to other cells in a network configuration. In contrast, in cells transfected with ANGPTL7/CDT6, fibronectin appears to be unable to form fibrils to the same extent seen in the mock-transfected ones (Fig. 4). Instead, the extracellular fibronectin in the transfected cells dish exhibited a discontinuous pattern that remained attached to the surface and did not form a fibril network. The overall levels of ECM fibronectin in the cells overexpressing ANGPTL7/CDT6 were also diminished. As fibronectin is a key organizer and signaling molecule of the ECM (Faralli *et al.* 2009) in the trabecular meshwork, we next assessed whether the altered fibronectin would

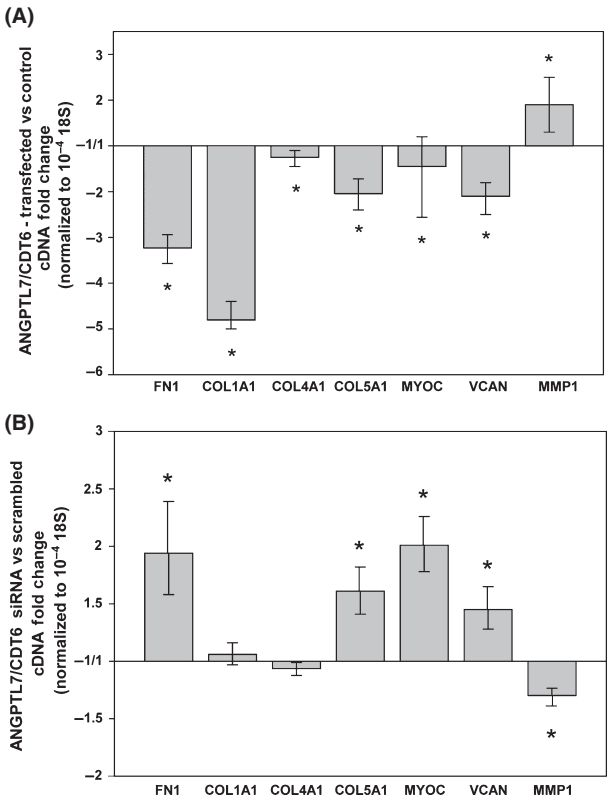

Figure 2 Effect of overexpressing and silencing ANGPTL7/CDT6 gene on the expression of extracellular matrix (ECM) relevant proteins in primary human trabecular meshwork cells, analyzed by real-time *Taq*Man PCR and expressed as fold change mean ± range. (A) Fold changes of ECM relevant genes in cells transfected with ANGPTL7/CDT6 cDNA over mock negative control ($n = 3$; $\star P \leq 0.03$). (B) Expression of ECM relevant genes in cells transfected with ANGPTL7/CDT6 siRNA over scrambled siRNA control ($n = 3$; $\star P \leq 0.03$). Overexpression of ANGPTL7/CDT6 significantly decreases all tested ECM genes with the exception of MMP1. Silencing of ANGPTL7/CDT6 significantly increases the expression of relevant ECM genes and decreases the expression of MMP1.

have a downstream effect on the formation of stress fibers. After the fibronectin antibody reaction, HTM cells were permeabilized and stained with rhodamine-conjugated phalloidin. Although a fully actin network disruption was not observed, the formation of stress fibers was clearly compromised (Fig. 4). The fact that ANGPTL7/CDT6 can modulate fibronectin matrix assembly suggests that levels of this protein could have profound consequences on the overall structure, support, and flexibility of the ECM.

Altogether these results suggest that ANGPTL7/CDT6 had a direct effect on the production and configuration of structural ECM proteins.

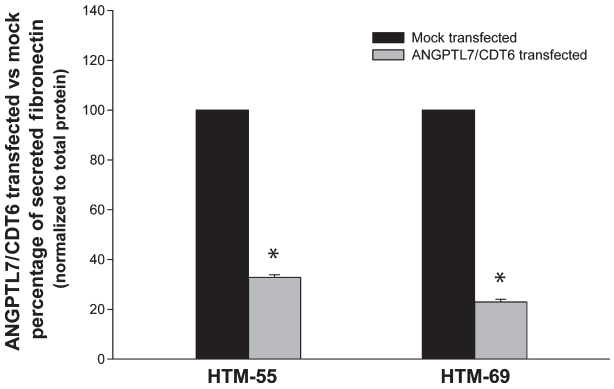

Figure 3 Effect of overexpressing ANGPTL7/CDT6 gene cells on secreted fibronectin of trabecular meshwork cells. Cell culture media from two primary cell lines mock and ANGPTL7/CDT6 nucleofector transfected were harvested at 72-h post-transfection. Soluble secreted Fibronectin was quantified by ELISA as indicated in methods. Reductions of fibronectin in treated samples are expressed as a percentage from the mock-transfected controls (mean ± SEM; $n = 3$; $\star P < 0.0001$). Secreted fibronectin is significantly reduced in trabecular meshwork cells overexpressing ANGPTL7/CDT6.

Influence of ANGPTL7/CDT6 on the DEX induction of trabecular meshwork proteins

Several reports in the literature (Rozsa *et al.* 2006; Nehme *et al.* 2009), including those from our own laboratory (Lo *et al.* 2003; Borrás 2008b) have shown that ANGPTL7/CDT6 is perhaps the highest DEX-induced gene in the human trabecular meshwork. Because DEX is an important trigger of hypertension (Armaly & Becker 1965; Kitazawa & Horie 1981), and because DEX specifically upregulates the glaucoma-associated gene myocilin, we sought to determine whether ANGPTL7/CDT6 might have a role in mediating the DEX response of other genes in the trabecular meshwork cells. For that, we aimed to silence the DEX induction of ANGPTL7/CDT6 with siRNA. Primary HTM cells were presilenced by nucleofector transfection of 2 μg of either scrambled control or ANGPTL7/CDT6 siRNA and treated with DEX 24 h later. At 48-h post-DEX, cells were harvested for expression analysis of trabecular meshwork ECM genes. Parallel wells of HTM cells nucleofector transfected with either ANGPTL7/CDT6 siRNA or a scramble siRNA control were left untreated for determination of DEX induction. In the presence of the scramble control, ANGPTL7/CDT6 cDNA was induced 30.3-fold (26/35.3 range) in the DEX- vs. vehicle-treated cells; when silenced by the presence of its own siRNA, the

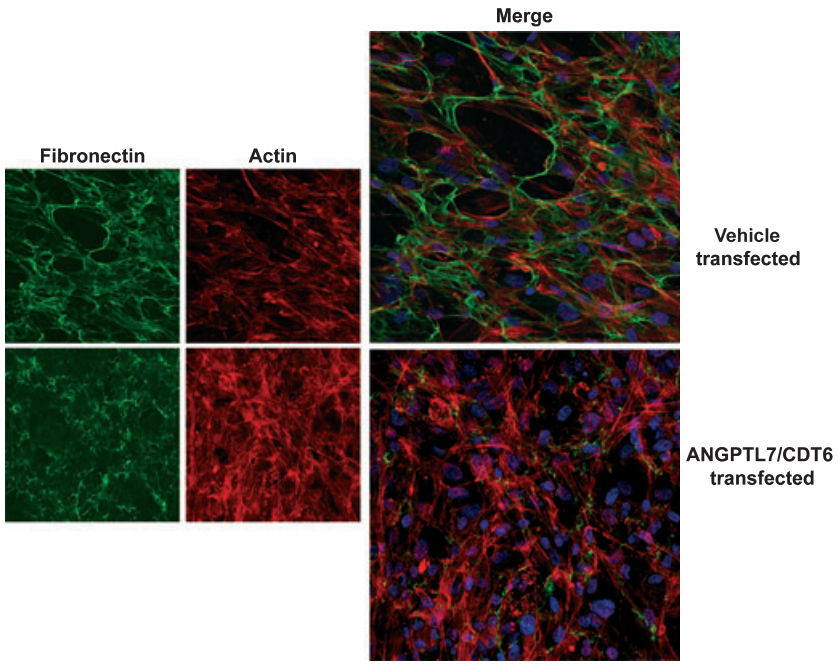

Figure 4 Effect of overexpressing ANGPTL7/CDT6 on fibronectin assembly. Primary HTM cells were grown for 4.5 days after mock and ANGPTL7/CDT6 nucleofector transfection. Cells were then fixed and processed for FN1 immunofluorescence under nonpermeabilized conditions followed by rhodamine-conjugated phalloidin under permeabilized conditions. Cells were stained with a mouse anti-human fibronectin primary antibody (1 : 100) and an Alexa 594-conjugated donkey anti-mouse secondary antibody (1 : 1000). Subsequently, cells were permeabilized and stained with rhodamine-conjugated phalloidin (1 : 500). Fluorescence images from vehicle and ANGPTL7/CDT6 transfected cells were taken at the same resolution, zoom, pinhole size, and amplitude offset on a confocal laser scanning microscopy with a 40× objective. Pictures were arranged using Adobe Photoshop.

upregulation was reduced to 6.6-fold (4.8/9.2 range). This 4.6× ($P = 0.03$) decrease in levels of ANGPTL7/CDT6 mRNA and/or protein in the silenced cells did affect the DEX induction of all ECM genes in this study. All ECM genes were either less upregulated, or more downregulated upon silencing of ANGPTL7/CDT6 induction. The most affected gene was FN1 whose DEX-upregulation was reduced 3.4× ($P = 0.001$), followed by MYOC whose reduction was 2.3× ($P = 0.004$). The remaining genes were reduced 1.5× (COL1A1, $P = 0.093$), 1.3× (COL4A1, VCAN and MMP1, $P = 0.13$, 0.28, and 0.06 respectively), and 1.2× (COL5A1, $P = 0.17$). The experiments were repeated in a different primary cell line with a similar outcome. A 6.5× ($P = 0.001$) reduction of ANGPTL7/CDT6 provoked a significant reduction of FN1 (1.5×, $P = 0.03$), MYOC (1.4×, $P = 0.003$), VCAN (1.2×, $P = 0.01$), and MMP1 (1.8×, $P = 0.02$). Although not significantly, the collagen encoding genes were also reduced: COL4A1 (2.2×, $P = 0.05$), COL1A1 (1.5×, $P = 0.1$), and COL5A1 (1.2×, $P = 0.17$) (Fig. 5).

Effect of silencing ANGPTL7/CDT6 on perfused human anterior segments

To best mimic an *in vivo* physiologic situation, and to confirm findings obtained on primary cells, we studied the effects of ANGPTL7/CDT6 in an intact human trabecular meshwork. We used the anterior segment–perfused organ culture system set up with paired eyes from postmortem human donors, as described in methods. In this organ culture procedure (Fig. 6A), the trabecular meshwork conserves its original architecture and is subjected to similar pressure conditions as those encountered in a living individual. In addition, the procedure allows the comparison of two human eyes from the same individual, and thus, results are not confounded by different genetic backgrounds. Because of our ability to deliver naked siRNA to the trabecular meshwork in this system (Comes & Borrás 2007), we perfused one eye of each pair with 100 nM of ANGPTL7/CDT6 siRNA whereas the contralateral eye was perfused with 100 nM of a scrambled siRNA control (Fig. 6A). We

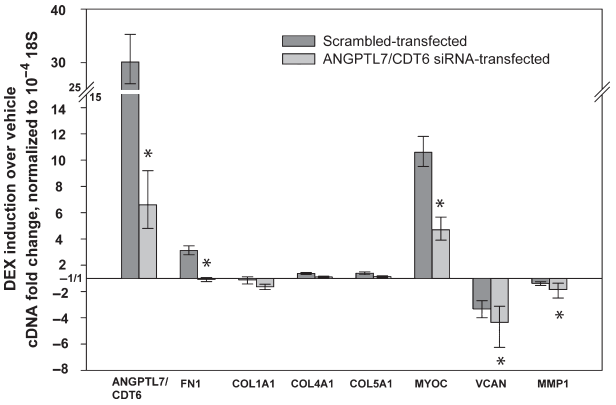

Figure 5 Effect of ANGPTL7/CDT6 silencing during dexamethasone (DEX) induction of human trabecular meshwork cells. Primary trabecular meshwork cells were nucleofector-transfected with ANGPTL7/CDT6 siRNA and scrambled control. At 24-h post-transfection, cells were treated either with DEX or vehicle for 48 h. Fold change expression of extracellular matrix relevant genes in DEX over vehicle treated was determined for both, ANGPTL7/CDT6 and scrambled siRNA transfected cells. Fold changes of each group were normalized to its endogenous 18S and expressed as mean ± range ($n = 3$; $\star P \leq 0.03$). Silencing of ANGPTL7/CDT6 reduces the induction of FN1 and MYOC genes and increases the DEX-downregulation of VCAN and MMP1. ANGPTL7/CDT6 mediates DEX induction of trabecular meshwork relevant genes.

carried out the experiment in the absence and presence of DEX and measured the levels of secreted MYOC protein at 24- and 48-h post-treatment. At the end of the experiment, we either dissected the trabecular meshwork tissue to measure gene expression and/or process wedges for immunohistochemistry. Three eye pairs from nonglaucomatous postmortem donors were perfused at 4 μL/min constant flow. The DEX experiment was pretreated with siRNA for 24 h followed by a combination of siRNA and 0.1 μM DEX for an additional 48 h.

In the absence of DEX, the mRNA levels in the ANGPTL7/CDT6 siRNA-perfused eye over the scrambled siRNA-perfused one and normalized with 18S were: −1.34 ± 0.13-fold for ANGPTL7/CDT6, 1.24 ± 0.13-fold for MYOC and 2.10 ± 0.23-fold for FN1 (eye #1, $n = 3$, $P = 0.02$, 0.04 and 0.002 respectively) (Fig. 6B, left). Equivalent aliquots from 1.7× concentrated effluents from eye #2 analyzed by a MYOC Western blot showed that the MYOC band intensities were higher in the eye perfused with ANGPTL7/CDT6 (Chan 1, Fig. 6B, right) than in the scramble control (Chan 2, Fig. 6B, right) at both time points.

In the presence of DEX, the mRNA levels in the ANGPTL7/CDT6 siRNA-perfused eye over the scrambled siRNA-perfused eye and normalized with 18S were: −7.90 ± 0.50-fold for ANGPTL7/CDT6, −2.50 ± 0.46-fold for MYOC and −1.36 ± 0.06-fold for FN1 (eye #3, $n = 3$, $P = 0.00006$, 0.002 and 0.000002 respectively) (Fig. 6C, left). Equivalent aliquots from 1.7× concentrated effluents from the same eye pair analyzed by a MYOC Western blot showed that the MYOC band intensities were lower in the eye perfused with ANGPTL7/CDT6 (Chan 1, Fig. 6C, right) than in the scramble control (Chan 2, Fig. 6C, right) at both time points.

The increase in MYOC upon treatment with ANGPTL7/CDT6 siRNA could also be observed by immunohistochemistry of the trabecular meshwork tissue by MYOC labeling of sections from opposite quadrants from eye pair #1 (Fig. 7, top). Quantification of the intensity of MYOC staining in the region of the trabecular meshwork using MetaMorph software showed that for the same area of 208,676 pixels, the measure intensity of the ANGPTL7/CDT6 siRNA treated eye had a higher value than the control, with intensity values of 17,608,077 and 9,562,985, respectively. Morphology images of the same eyes, stained with H&E, show that the architecture is well preserved and that the tissue conserved the canonical layered trabecular meshwork structure and SC (Fig. 7, bottom). In these images, taken into account the limitations of light microscopy resolution, the treated eye appears to have a wider ECM tending to constrict the Schlemm's canal.

Discussion

Our interest on the relevance of ANGPTL7/CDT6 gene (called CDT6 in our earlier publications) in the trabecular meshwork was sparked by the high inducibility of this gene in the aqueous humor outflow tissue under conditions associated with glaucoma. Our recent publication comparing the relative abundance of 21 most relevant genes with their pressure inducibility in a perfused organ culture system showed that ANGPTL7/CDT6 was the gene with the highest pressure-inducibility/abundance ratio (Comes & Borrás 2009). Although it has not been directly calculated, this high degree of inducibility appears to also hold for DEX and TGFβ2 inductions (Lo *et al.* 2003; Zhao *et al.* 2004; Rozsa *et al.* 2006). The abundance of ANGPTL7/CDT6 in the trabecular meshwork is relatively low compared to its abundance in the cornea, as shown in our perfused

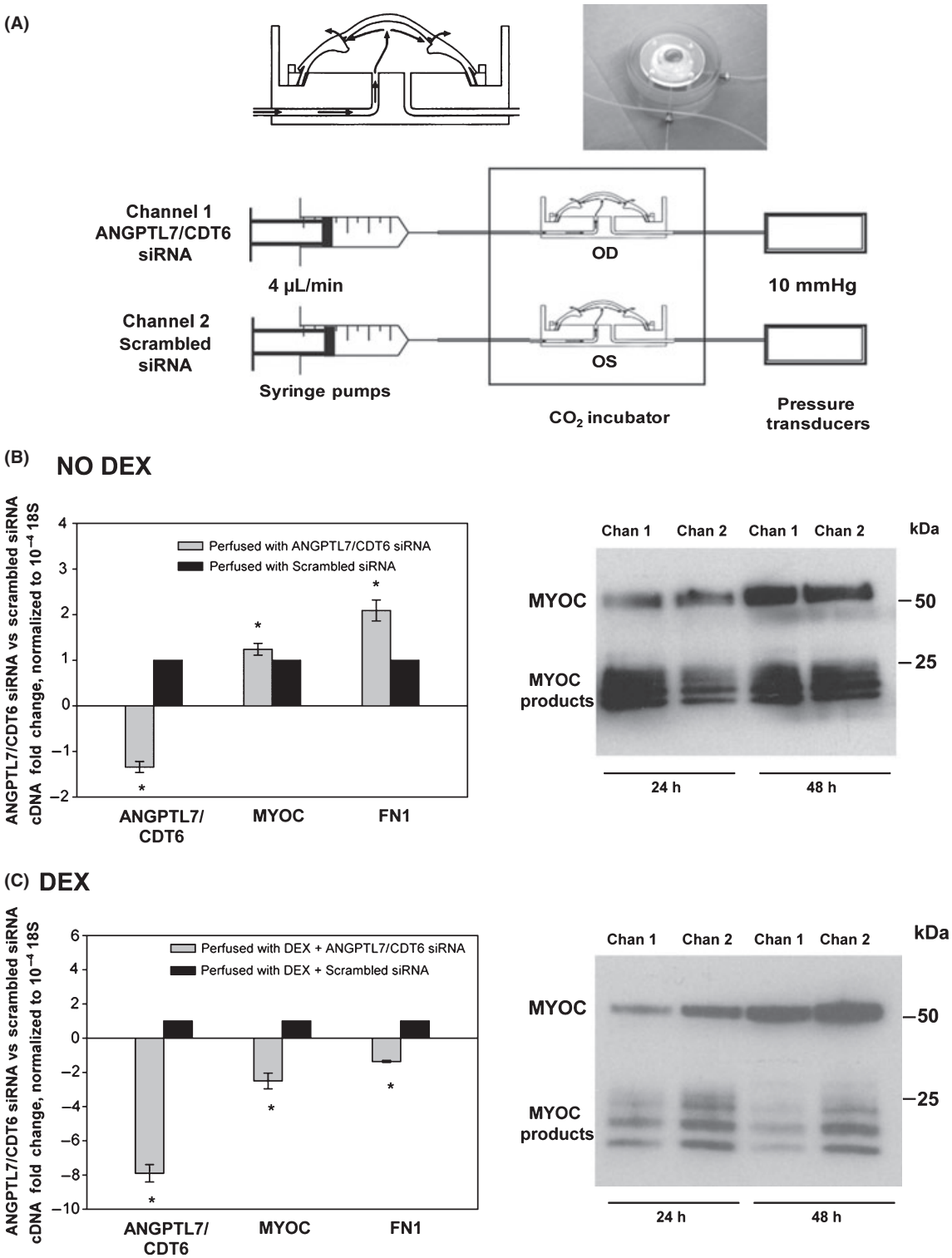

tissue cDNA library (Peek *et al.* 1998; Gonzalez *et al.* 2000) and in the recent immunohistochemistry study of Kuchtey (Kuchtey *et al.* 2008). A higher abundance was reported in the National Eye Institute library (15th most abundant gene) (Tomarev *et al.* 2003b), but it is possible that this high expression had

Figure 6 Effect of ANGPTL7/CDT6 silencing in a perfused, intact human trabecular meshwork in the absence and presence of dexamethasone (DEX). (A) Schematic representation of the perfused human anterior segment organ culture. *Top left:* diagram of the custom made perfusion chamber; *Top right*: actual photograph of a postmortem human anterior segment mounted to the chamber (a mounting ring holds the tissue in place and provides a leak-proof seal). *Bottom:* diagram of the perfused system; the culture chambers are maintained at 37 °C in a CO_2 environment; culture medium is perfused using a microinfusion syringe pump at 4 μL/min; the right eye (channel 1) was perfused with 100 nM solution of ANGPTL7/CDT6 siRNA, whereas the left eye (channel 2) received 100 nM of Scrambled siRNA. The trabecular meshwork tissue was dissected at the end of the experiment and harvested for RNA and *Taq*Man assays. Effluents were collected at 24- and 48-h post-treatment and processed for the analysis of secreted MYOC. (B) *Left:* fold changes of ANGPTL7/CDT6, MYOC and FN1 in ANGPTL7/CDT6- versus Scrambled siRNA, normalized to 18S and expressed as mean ± SEM. Upon normalization, the Scrambled control is given a value of 1 (eye pair #1, $^{\star}P < 0.04$). *Right*: equivalent aliquots of concentrated effluents analyzed by Western blot with a goat anti-human MYOC antibody (eye pair #2). (C) Eyes were pretreated with the siRNAS for 24 h followed by siRNAs/DEX for 48 h. *Left:* fold changes of ANGPTL7/CDT6, MYOC and FN1 in ANGPTL7/CDT6- versus Scrambled siRNA, normalized to 18S and expressed as mean ± SEM. Upon normalization, the Scrambled control is given a value of 1 (eye pair #3, $^{\star}P < 0.002$). *Right*: equivalent aliquots of concentrated effluents analyzed by Western blot with a goat anti-human MYOC antibody at 24- and 48-h post-DEX treatment (eye pair #3). Silencing ANGPTL7/CDT6 in the intact TM induces the expression of FN1 and MYOC. Silencing ANGPTL7/CDT6 in the intact TM during DEX treatment interferes with the DEX induction of FN1 and MYOC.

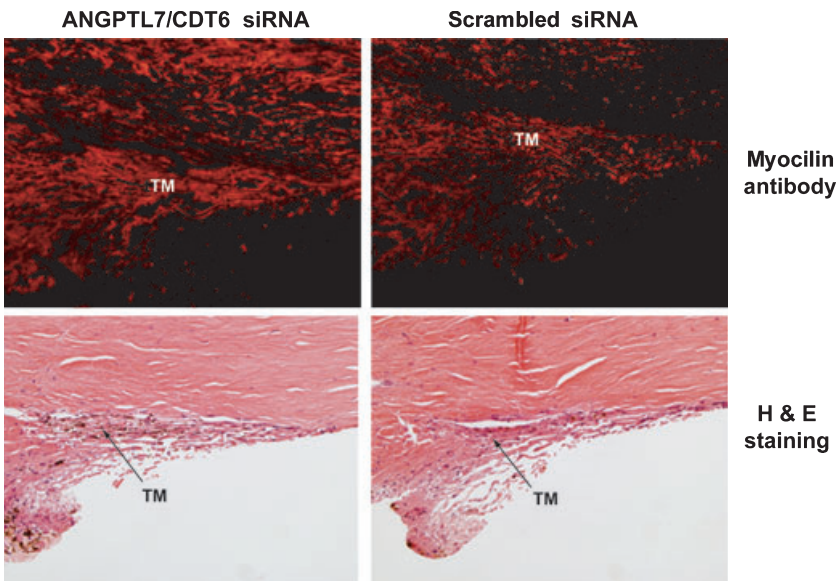

Figure 7 Histologic assessment of human trabecular meshworks from anterior segments perfused with ANGPTL7/CDT6 and Scrambled siRNA. *Top*: MYOC expression examined by immunohistochemistry on OCT-embedded frozen sections from blocks containing tissue wedges from opposite quadrants of eye pair #1. Ten-micrometer sections were stained with goat anti-human MYOC and donkey anti-goat Alexa Fluor 594. *Bottom*: 5-μm paraffin sections from opposite quadrants of the same eye pair stained with H&E. Quantification of fluorescence intensity showed that MYOC expression is higher in the eye perfused with ANGPTL7/CDT6 siRNA than in the contralateral eye perfused with Scrambled siRNA. Although the architecture of the trabecular meshwork is well conserved in both eyes, the eye perfused with ANGPTL7/CDT6 siRNA appears to have more extracellular matrix that tends to constrict the Schlemm's canal.

been influenced by the medication (very often, steroids) of the patients at the time of death and eye procurement.

Regarding pressure induction, the presence of four TCF/LEF transcription factor–binding sites in the 5′-flanking promoter region of ANGPTL7/CDT6 (Katoh & Katoh 2006) is very intriguing. These transcription factors are key for the activation of the WNT/β-catenin signaling pathway (Cadigan 2008), and this pathway has been recently connected with elevated IOP and glaucoma (Wang *et al.* 2008; Comes & Borrás 2009). The WNT secreted

glycoproteins transmit signals by binding to frizzled transmembrane receptors. This binding results in the dephosphorylation and nuclear translocation of β-catenin, which in turn activates gene expression by interacting with transcription factors of the TCF/LEF family. Array data from our laboratory and others have shown that the trabecular meshwork expresses a number of WNT signaling-related genes (Borrás 2008a; Wang *et al.* 2008; Comes & Borrás 2009). In addition, WNT antagonists *secreted frizzle-related protein 4* (SFRP4) and *secreted frizzle-related protein 1* (SFRP1) are induced by elevated pressure (Comes & Borrás 2009), and SFRP1 expression is elevated in glaucomatous HTM cells (Wang *et al.* 2008). It would, then, be possible to think that the activation of ANGPTL7/CDT6 by elevated IOP could be mediated by the activation of the cis-acting WNT regulatory elements. ANGPTL7/CDT6 is inserted in an intron of the MTOR gene in the antisense orientation (Katoh & Katoh 2006); thus, it is unlikely that its expression and induction by elevated IOP would be affected by the expression of the 'parent' gene. A look into our trabecular meshwork pressure array collection showed that, although the MTOR gene (alias FRAP1 and FRAP2) is expressed in the tissue, it is not altered by elevated IOP (unpublished results).

To study the effect of overexpressing and silencing ANGPTL7/CDT6 on matrix production, we rationally selected a group of ECM proteins known to be relevant to outflow facility function. We found that elevated intracellular levels of ANGPTL7/CDT6 reduced expression of fibronectin, collagen type IA1, collagen type VA1, versican and to a lesser extent collagen type IVA1 and myocilin. In contrast, the expression of MMP1 was induced. When we silenced trabecular meshwork ANGPTL7/CDT6 expression with its siRNA, the subsequent expression of the same ECM genes was reversed.

Fibronectin is one of the most important ECM proteins of the trabecular meshwork (Hann *et al.* 2001; Faralli *et al.* 2009). Soluble fibronectin is secreted by the cells, binds to the cell surface α5β1 integrin and assembles into fibrils around the periphery of the cells (Mao & Schwarzbauer 2005; Dallas *et al.* 2006). Fibronectin provides mechanical support to the trabecular meshwork tissue, and changes in its expression have been observed in glaucoma patients (Hann *et al.* 2001) as well as under conditions that would lead to increased resistance (Faralli *et al.* 2009). Its different binding domains, which bind to the integrin receptors and to ECM proteins, have been implicated in modifying outflow facility characteristics such as signal transduction, cell attachment, and cell contraction (Faralli *et al.* 2009).

In this study, transcription of fibronectin was decreased by ANGPTL7/CDT6 overexpression and this reduction was reversed by the silencing of the gene. Secreted fibronectin was also diminished in ANGPTL7/CDT6-transfected cultures. Furthermore, in these cultures, the formation of fibronectin in fibrils was altered, showing a more punctate pattern and a lack of network formation. These changes seemed to have a downstream effect on the actin network and could influence outflow facility. Because increases in fibronectin have been mostly associated with characteristics that increase outflow resistance (Faralli *et al.* 2009), one would speculate that overexpression of ANGPTL7/CDT6 tends to facilitate rather than obstruct aqueous humor outflow. In other words, the induction of ANGPTL7/CDT6 observed with DEX, TGFβ2, and elevated IOP (Lo *et al.* 2003; Zhao *et al.* 2004; Borrás 2008b; Comes & Borrás 2009; Nehme *et al.* 2009) could be the reflection of a counteractive or defense mechanism against elevated IOP instead of a detrimental one. This hypothesis is supported by the results on the effects of ANGPTL7/CDT6 on MMP1 expression. In the same RNA samples where fibronectin was reduced, MMP1 was elevated; correspondingly, when fibronectin was increased, MMP1 was reduced. MMP1 is an interstitial collagenase that breaks down ECM collagens. This enzyme has been widely studied in the trabecular meshwork and it has been shown to increase outflow facility in organ cultures (Bradley *et al.* 1998), to be upregulated by glaucoma drugs (Hinz *et al.* 2005), and to reduce IOP in living animals (Gerometta *et al.* 2010).

Fibronectin (secreted and surface-associated fibronectin) is also downregulated in cells overexpressing myocilin (Shen *et al.* 2008). As overexpression of ANGPTL7/CDT6 reduced myocilin, and silencing ANGPTL7/CDT6 increased its expression, it would seem that the effects of ANGPTL7/CDT6 on fibronectin expression are of a direct nature and override the effects of myocilin on fibronectin (on this protein). Experiments simultaneously overexpressing and/or silencing ANGPTL7/CDT6 and myocilin would help to elucidate a potential synergy between both genes.

Our results on collagen type I mRNA do apparently disagree with the higher levels of the collagen deposition observed in ANGPTL7/CDT6 stably transformed cells (Kuchtey *et al.* 2008). This could perhaps be because of the difference of using transformed versus primary trabecular meshwork cells, or that collagen

type I is subjected to a post-transcription regulation in these cells.

ANGPTL7/CDT6 overexpression reduced total versican transcription. Although some splicing isoforms of versican were reported to be upregulated, total versican expression was shown to be reduced after subjecting trabecular meshwork cells to mechanical stretch (Keller *et al.* 2007). Versican is a chondroitin sulfate glycosaminoglycan that binds to fibronectin and several other ECM components (Wight 2002). It comprises a high portion of the chondroitin sulfates in the trabecular meshwork, and it is known to contribute to outflow resistance and to be elevated in glaucoma patients (Knepper *et al.* 1996, 2005). Thus, a reduction in versican would lead to an unbalance in the organizational structure of the ECM in a manner that could facilitate the flow of aqueous humor.

Studies from our laboratory and those of others have shown the high inducibility of ANGPTL7/CDT6 by the glucocorticoid DEX. Glucocorticoids are potent immunosuppressants that induce ocular hypertension in steroid-responsive patients (Armaly & Becker 1965; Kitazawa & Horie 1981). However, the genes and mechanisms of steroid glaucoma are not well understood. Here, by comparing DEX-scrambled to vehicle-scrambled, and separately, DEX-ANGPTL7/CDT6 siRNA to vehicle-ANGPTL7/CDT6 siRNA, we are able to look at the effect of ANGPTL7/CDT6 on the glucocorticoid induction of other ECM genes. We find that reducing the high levels of ANGPTL7/CDT6 during DEX treatment affects the induction of other ECM landmark genes, such as myocilin, fibronectin, versican, and MMP1. These results suggest that ANGPTL7/CDT6, in addition to influencing directly the expression of the ECM genes (Fig. 2), is also affecting their induction by the glucocorticoid (Fig. 5). Whether these two functions are connected is not yet clear.

In summary, our studies of the effect of ANGPTL7/CDT6 on the ECM of the trabecular meshwork show that this member of the angiopoietin-like protein family might play an important role in the deposition and organization of the matrix of the outflow tissue. Furthermore, they show that interference with ANGPTL7/CDT6 induction by glucocorticoids significantly affects the induction of key glaucoma-related proteins, such as fibronectin, myocilin, versican, and MMP1. These findings, together with our previous results on its upregulation by elevated IOP (Comes & Borrás 2009), establish this gene-protein as a strong candidate for a potential management of glaucoma.

Experimental procedures

Primary cultures of outflow pathway cells

Primary cell lines HTM-41 and HTM-55 were generated, respectively, from the eye pairs of 18- and 25-year-old nonglaucomatous human donors obtained from the Lions Eye Bank of Oregon and National Disease Research Interchange after signed consent of the patients' families. All procedures were in accordance with the Tenets of the Declaration of Helsinki. For isolation of HTM cells, the trabecular meshwork was isolated from surrounding tissue under a dissecting microscope by making incisions both anterior and posterior to the meshwork and removing it using forceps. The tissue was then cut into small pieces and treated with 1 mg/mL collagenase type IV (Worthington, Lakewood, NJ, USA) in Phosphate-Buffered Saline (PBS, Invitrogen-Gibco) and incubated at 37 °C in a shaker water bath for 1 h as described (Vittitow & Borrás 2004). Incubation was followed by low-speed centrifugation for 5 min. Pellet was resuspended in 4 mL of Improved Minimal Essential Medium (IMEM; Biofluids) supplemented with 20% Fetal Bovine Serum (FBS; Invitrogen-Gibco) and 50 μg/mL gentamicin (Invitrogen-Gibco). Resuspended tissue was plated on a single, 2% gelatine-coated 35-mm dish and maintained in a 37 °C, 7% CO_2 incubator. The medium was changed every other day and once confluent (2–3 weeks), cells were passed to a T-25 flask and labeled as a passage 1. Subsequently, cells were passed 1 : 4 at confluency and maintained in the same medium with 10% FBS (complete IMEM). The HTM-69 and HTM-137 cell lines were generated, respectively, from the trabecular meshworks dissected from residual cornea rims of 29- and 39-year-old donors after surgical corneal transplants at the University of North Carolina Eye Clinic. The tissue was cut into small pieces, carefully attached to the bottom of the 2% gelatine-coated 35-mm dish, and covered with a drop of IMEM medium supplemented with 20% FBS and 50 μg/mL gentamicin and a cover slip. Cells from this specimen were not treated with enzymes and were allowed to grow from the explant for a period of 4 weeks changing the media every other day; upon confluency, cells were treated as described. These primary nontransformed cells subsist for nine to ten passages. In this study, all cells were used at passage 5. These outflow pathway cultures comprise all cell types involved in maintaining resistance to flow. These include cells from the three distinct regions of the trabecular meshwork plus cells lining the Schlemm's canal. Because most of the cells in these cultures come from the trabecular meshwork, they are commonly referred to as 'trabecular meshwork cells'.

Generation of the ANGPTL7/CDT6 expression vector

Human ANGPTL7/CDT6 cDNA was amplified by PCR from primary HTM cells (HTM-41) treated with DEX for 10 days. Total RNA, extracted as indicated in the following paragraphs, was reverse transcribed using the RETROscript kit

(Ambion). Briefly, 1 μg of total RNA was mixed with 2 μL of 50 μM random decamers in a total of 12 μL, heated at 75 °C for 2 min and cooled on ice. The reaction continued in a 20-μL mix containing 2 μL of 10× RT buffer, 4 μL dNTP (2.5 μM each), 1 μL RNase inhibitor (10 U), and 1 μL M-MuLV reverse transcriptase (100 U). The reaction mixture was incubated at 42 °C for 60–90 min and terminated at 92 °C for 2 min. ANGPTL7/CDT6 cDNA amplification was carried using forward 5′-CAC CCA AAC CCA CAA AAG ATG CTG-3′ and reverse 5′-TTA AGG CTT GAA GTC TTC TGG GCG-3′ specific primers, yielding an amplification product of 1058 bp (231–1280 nt in gene bank sequence access number NM_021146). PCR was carried out in a 50-μL reaction mixture containing 5 μL 10× high-fidelity PCR buffer, 1 μL dNTP (10 μM each), 2 μL $MgSO_4$ (50 μM), 4 μL primers (5 μM each), 1 μL template cDNA and 1 μL Platinum® *Taq* High Fidelity DNA Polymerase (5 U) (Invitrogen). Amplification was carried out at 94 °C for 4 min, 38 cycles of 94 °C for 30 s, 55 °C for 1 min, 72 °C for 30 s, and a final extension at 72 °C for 7 min. PCR products were electrophoresed on a 1.5% SuperAcryl agarose gel containing 25 ng/mL ethidium bromide, gel purified, sequenced, and cloned into pcDNA 3.1.V5-His-TOPO® TA expression vector (Invitrogen). The resulting plasmid, pNC1, was restricted and re-sequenced to confirm orientation and reading frames. Plasmid DNA was isolated using a Midi-Prep plasmid kit (QIAGEN) and further purified by double binding in a cesium chloride gradient. Alternatively, plasmid DNA was purified using the Power Prep Express PCR Purification kit (Origene), which resulted in lower toxicity after the nucleofector transfection (not shown).

Nucleofector transfection of primary HTM cells

Human ANGPTL7/CDT6 was transfected to cultured primary HTM cells using nucleofector technology (Amaxa Lonza) and their basic kit from Primary Mammalian Endothelial Cells according to manufacturer's directions. Pilot experiments with 4×10^5 nontransformed HTM cells and 2 μg of pMax green fluorescent protein plasmid provided in the kit were used to determine conditions for maximum transfection efficiency. Of the built-in programs, program T-23 was found to result in an approximate 80% efficiency viability for HTM cells (not shown); thus, it was selected for consecutive studies. For this transfection procedure, cells were split 24 h before transfection to obtain 70–80% confluency. Cells were then trypsinized, counted with a hemacytometer (Hausser Scientific), and centrifuged at 100 ***g*** for 10 min. Cell pellets were resuspended in full strength proprietary mammalian endothelial solution provided in the kit at a concentration of 4×10^5 cells/100 μL. Upon the addition of approximately 0.5 μL (2 μg) of ANGPTL7/CDT6 or equivalent volume of H_2O as a control, the cell-DNA mix was electroporated on the nucleofector apparatus (Amaxa Lonza) using program T-23. Immediately after electroporation, the cell-DNA solution was allowed to recover for 15 min in the CO_2 incubator, inside an eppendorf tube containing 0.5 mL of prewarmed complete IMEM medium. After the recovery period, cells were gently transferred to warm medium-containing 3-cm dishes. Twenty-four hours after transfection, media was changed and subconfluent HTM cells were maintained in IMEM medium in the presence of serum for an additional 48 h. Transfected cells were washed 2× with PBS and scraped from the dish using 350 μL guanidine thiocyanate buffer (RLT; QIAGEN). Cells were then processed for RNA extraction as indicated in the following paragraphs.

RNA extraction and reverse transcription reaction

RNA extraction was carried out by resuspending cellular pellets in 350 μL of guanidine thiocyanate buffer (RLT; QIAGEN) and loading the homogenized solution onto a QIAshredder™ column (QIAGEN). The extraction continued by the use of the RNeasy Mini kit with RNase-free DNase digestion on the column provided according to manufacturer's recommendations (QIAGEN). Total RNA recoveries averaged 2.6 ± 0.06 μg per 3-cm dish culture. Reverse transcription (RT) reactions and followed-up normalized cDNA quantification were carried out by real-time *Taq*Man PCR technology (Applied Biosystems, ABI). For the real-time *Taq*Man PCR procedure, the RT reactions were conducted with approximately 1 μg of spectrophotometrically measured total RNA in a 25 μL total volume of proprietary RT buffer containing random primers, dNTPs and 62.5 U of Multiscribe MuLV RT enzyme with RNAse inhibitor (High Capacity cDNA kit; ABI) following manufacturer's recommendations (25 °C 10 min, 37 °C 2 h).

Transfection of short-interfering RNA on primary HTM cells

The Silencer® predesigned human ANGPTL7/CDT6 siRNA (ID number 121883) and nontargeted scramble Silencer® Negative Control number 1 siRNA (catalog number 4635) were synthesized by Ambion. The siRNA sense and antisense sequences targeting ANGPTL7/CDT6 (GenBank NM_021146) were 5′-GCA CAA GAC ACC AGC ACA Gtt-3′ and 5′-CUG UGC UGG UGU CUU GUG Ctt-3′, respectively. ANGPTL7/CDT6 siRNA was reconstituted to a final concentration of 100 μM in 200 μL of RNAse-free water and stored in aliquots at −20 °C. The negative control siRNA was comprised of a 19-bp (base pair) scrambled sequence and was reconstituted in the same manner but to a final concentration of 50 μM.

Primary HTM cells were transfected with siRNAs also using the nucleofector technology described earlier. Volumes of 1.2 μL or 2.4 μL from ANGPTL7/CDT6 siRNA (100 μM) or scramble siRNAs (50 μM) respectively, were mixed with 4×10^5 cells in 100 μL of endothelial media, electroporated, let to recover and transferred to 3 mL full IMEM medium. Final siRNA concentration in the subconfluent dishes was

27 nM. Twenty-four hours after transfection, media was changed and HTM cells treated with DEX for 48 h in the presence of serum followed by an additional 24 h serum-free medium containing DEX or vehicle. Dexamethasone (DEX; Sigma) stock solution was prepared by adding absolute ethanol to the commercial vial obtaining a final concentration of 0.1 mM and kept at 4 °C. The DEX stock solution of 0.1 μM was diluted 1000× (100 nM final concentration) in IMEM media before use. Parallel dishes received IMEM medium containing the drug vehicle under the same conditions. At the end of each treatment, cells were washed two times with PBS, lysed with 350 μL guanidine thiocyanate buffer and processed for RNA extraction as indicated earlier.

Quantification of gene expression by Real-Time *Taq*Man PCR

Normalized cDNA quantification was carried out by real-time *Taq*Man PCR (ABI). For that, fluorescently labeled *Taq*Man probes/primers sets of selected genes were purchased from the ABI *Taq*Man Gene Expression collection (http://www.allgenes.com). The ANGPTL7/CDT6 probe corresponded to sequences from exons 1 and 2 (Hs00221727_m1), FN1 probe corresponded to sequences from exons 40 and 41 (Hs00415006_m1), COL1A1 probe corresponded to sequences from exons 1 and 2 (Hs00164004_m1), COL4A1 probe corresponded to sequences from exons 20 and 21 (Hs00266237_m1), COL5A1 probe corresponded to sequences from exons 16 and 17 (Hs00609088_m1), MYOC probe corresponded to sequences from exons 2 and 3 (Hs00165345_m1), CSPG2 probe corresponded to sequences from exons 3 and 4 (Hs00171642_m1), MMP1 probe corresponded to sequences from exons 6 and 7 (Hs00233958_m1), and the 18S rRNA probe corresponded to sequences surrounding position nucleotide 609 (Hs99999901_s1). Reactions were carried out in 20-μl aliquots using *Taq*Man Universal PCR Master Mix No AmpErase UNG (ABI), ran on an ABI Prism 7500 Real-Time PCR System Sequence Detection System (SDS) and analyzed by 7500 System SDS software (ABI). Relative Quantification (RQ) values between treated and untreated samples were calculated by the formula $2^{-\Delta\Delta C_T}$, where C_T is the cycle at threshold (automatic measurement), ΔC_T is C_T of the assayed gene minus C_T of the endogenous control (18S rRNA), and $\Delta\Delta C_T$ is the ΔC_T of the normalized assayed gene in the treated sample minus the ΔC_T of the same gene in the untreated one (calibrator). Because of the high abundance of the 18S rRNA, and in order to get a linear amplification, RT reactions from control and experimental samples were diluted 10^4 times before their hybridization to the 18S *Taq*Man probe. Relative quantification values >1 correspond to increased fold changes. Relative quantification values <1 correspond to a fraction of the gene expression and were converted to decreased fold changes by the formula $-1/2^{-\Delta\Delta C_T}$. That is, an RQ of four corresponds to an increased expression of 4-fold (+4), whereas an RQ of 0.25 corresponds to a reduction of expression of 4-fold (−4).

Western blot analysis

Human trabecular meshwork cells primary cells pretransfected with either H_2O (negative control) or human ANGPTL7/CDT6 were assayed for levels of ANGPTL7/CDT6 protein. Cultured cells were washed 2× with cold PBS pH 7.4 and scraped from the dish with 100 μL of modified RIPA buffer containing 1× protease inhibitor cocktail (Roche). Forty-eight-hour post-transfection serum-containing medium was replaced with serum-free medium. After 24 h, 4 mL of cell media from each condition were centrifuged at 470 ***g*** for 10 min to remove cellular debris. Cleared media containing secreted cell products were applied to NAP-10 columns (GE Healthcare Biosciences) to exchange the buffer to 0.1 M Tris-HCl pH7.4 (Sigma-Aldrich) and then concentrated (40×) with an Amicon Ultra-4 Filter Device (Millipore) at 2135 ***g***, 4 °C. Aliquots of 1.5 μL were mixed (1 : 2 vol) with Laemmli buffer (Bio-Rad) containing 5% β-mercaptoethanol and loaded onto 4–15% SDS–PAGE Tris-HCl polyacrylamide gels (Bio-Rad). After running, gels were electro-transferred to PVDF membranes (Bio-Rad), which were blocked with 5% nonfat dry milk (Bio-Rad) in PBS-0.2% Tween 20 (Sigma-Aldrich) for 2 h and incubated overnight at 4 °C with ANGPTL7/CDT6 goat polyclonal IgG antibodies (Proteintech Group) (1 : 200). Primary antibody reaction was followed by incubation with anti-rabbit IgG secondary antibodies conjugated with horseradish peroxidase (1 : 5000; Pierce Biotechnology) for 1 h at room temperature. Immunoreactive bands were visualized by chemiluminescence ECL Plus Western blotting detection system (GE Healthcare Biosciences) and membranes were exposed to light film (BioMax MR; Kodak). ANGPTL7/CDT6 bands from HTM cells overexpressed with ANGPTL7/CDT6 were captured using a ChemiDoc System equipped with a Chemi-cooled CCD camera, PCI digitizing image acquisition board, EpiChemi II Darkroom with transilluminator and LabWorks Software (UVP, Upland). Normalization for the distinct ANGPTL7/CDT6 bands intensities was subsequently carried out using the total protein concentration of each sample, which was measured using a Bradford Protein Assay (Bio-Rad).

For the organ culture, effluents were concentrated (1.7×), run, and processed as indicated earlier. Membranes were incubated overnight at 4 °C with a goat anti-human MYOC antibody (1 : 200; R&D Systems), washed, and incubated with anti-goat IgG secondary antibodies conjugated with horseradish peroxidase (1 : 2000; Pierce Thermo Fisher Scientific, Rockford, IL, USA) for 1 h at room temperature. Immunoreactive bands were visualized by chemiluminescence.

Quantification of fibronectin protein by ELISA

Soluble Fibronectin from human trabecular meshwork culture media was determined using the QuantiMatrix™ Human Fibronectin ELISA Kit (Millipore) following manufacturer's recommendations. This assay is in the format of a competitive inhibition ELISA and human fibronectin is precoated on the

wells of the strips in a 96-well microtiter plate holder. Fibronectin standard dilutions ranging from 3 ng/mL to 1000 ng/mL were prepared from a reconstituted stock solution (1 g/mL). Total protein of the cells medium was determined by the Bradford assay. Sixty μL of each experimental sample were used for the ELISA and the concentration of all samples fell within the range of the standard curve. Standards and samples were then preincubated for 10 min at room temperature with a solution containing polyclonal rabbit antibodies to human fibronectin. The mixtures were transferred in triplicates to the human fibronectin-coated plate previously rehydrated with washing buffer. After 1 h, the plate was rinsed and incubated with goat anti-rabbit IgG-HRP conjugated for 30 min at room temperature. TMB/E substrate was added to develop the color after washing. Reactions were stopped when the color of the highest concentration of the standard turned bright blue. The plate was read immediately at 450 nm using an automatic microplate reader (Fluostar Optima; BMG Labtechnologies, Cary, NC, USA). The fibronectin concentration of samples was interpolated from the standard curve values and normalized to total protein. As only free rabbit anti-human fibronectin from standards and samples binds to the fibronectin coated on the plate, the intensity of the color was inversely proportional to the amount of fibronectin in each sample.

Perfused human anterior segment organ cultures

Three pairs of normal, nonglaucomatous human eyes from donors ages 62–78 were obtained from national eye banks (North Carolina Eye Bank, NC; National Disease Research Interchange, (NDRI, PA) after signed consent of the patients' families. All procedures were in accordance with the Tenets of the Declaration of Helsinki. Whole eye globes within 24–40 h of death were dissected at the equator, cleaned and mounted on custom-made perfusion chambers as described previously (Borrás *et al.* 1999, 2002). Perfusion was conducted at constant flow at 4 μL/min with serum-free high glucose DMEM (Gibco Invitrogen) using a Harvard microinfusion pump (Harvard Bioscience). Pumps were controlled by a custom-made computer program (Infusion Pump Control Program, University of North Carolina Chemistry Department, Electronic Design Facility). Anterior segments were maintained at 37 °C, 5% CO_2 and perfused for 24 h to establish a stable baseline (steady pressure recordings for at least 10 h). The average outflow facility (*C:* flow/pressure in μL/min/mmHg) of the perfused eyes at baseline was $C = 0.19 \pm 0.04$ ($n = 5$). The sixth eye had a *C* of 1.55 as a result of a technical low pressure. Treatment was carried out by continuous perfusion of the siRNAs and/or combined DEX-siRNA diluted in DMEM perfusion medium. Final concentration of the siRNAs and DEX were 100 nM each. Fresh siRNA and/or DEX-siRNA were changed from the syringes every 24 h. Effluents were collected at the indicated times and saved at −20 °C until processed. At the end of the experiment, anterior segments were cut in several wedges that were either immersed in 4% paraformaldehyde, 4% paraformaldehyde/2.5% glutaraldehyde or RNA*later* (Ambion), for immunohistochemistry, morphology and gene expression.

Immunocytochemistry, immunohistochemistry, and light microscopy

Passage 4 primary HTM-137 cells at subconfluent density were nucleofector-transfected and immediately plated onto coated four-well glass chamber slides (Lab-Tek, Nalgene Nunc) at 62,500 cells/well. To coat the chamber slides, we added 2% porcine gelatin, and upon removal, incubated them overnight under UV light in a laminar flow hood. Cells were maintained in complete IMEM medium for 4.5 days to allow deposition of extracellular matrix. Cells were then washed 2× with PBS, fixed with fresh 4% paraformaldehyde in PBS for 5 min and washed three more times with PBS (5 min each wash). Non-permeabilized cells were blocked with 10% donkey serum for 20 min and incubated overnight at 4 °C with mouse anti-human fibronectin (BD Biosciences) at a 1 : 100 dilution in PBS/1.5% donkey serum. After primary antibody incubation, cells were washed, followed by staining with Alexa 594-labeled donkey anti-mouse (Invitrogen) for 1 h at room temperature and an additional wash. Subsequently, cells were permeabilized with 0.1% TritonX-100 in PBS for 5 min, washed, blocked in 10% goat serum for 20 min, washed, and stained with rhodamine-conjugated phalloidin (1 : 500; Sigma) for 1 h. An aliquot of a DAPI solution (final 1 : 1000×; Invitrogen) was added to the cells for the last 5 min. After washing, cells were mounted with Fluoromount-G (Southern Biotech), and same fields were imaged by confocal microscopy (SP2 AOBS; Leica). Confocal images for ANGPTL7/CDT6 transfected and controls were captured using the same resolution, zoom, pinhole size, and amplitude offset. Digital images were arranged with image analysis software (Photoshop CS; Adobe). Negative controls were run in parallel but incubated in 1.5% donkey serum PBS in place of the primary antibodies.

Tissue wedges from opposite quadrants of eye pair #1 were fixed by immersion overnight at room temperature in 4% paraformaldehyde in PBS for immunohistochemistry and in 4% paraformaldehyde/2.5% glutaraldehyde for morphology. For cryosections, specimens were consecutively washed in 10% sucrose (6 h), 30% sucrose (overnight) and frozen in Tissue-Tek OCT (Sakura Finetek, Torrance, CA, USA) in liquid nitrogen. Meridional 10-μm sections were mounted on charged Superfrost Plus microscope slides (Thermo Fisher Scientific). For the MYOC detection, sections were dried at room temperature and blocked with donkey serum for 1 h. Tissue sections were then incubated overnight at 4 °C with MYOC primary antibody (1 : 100 diluted in 0.3% TritonX-100, 7.5% donkey serum in PBS; R&D Systems) followed by incubation with donkey anti-goat Alexa Fluor 594 secondary antibody (1 : 500 diluted in 0.3% TritonX-100, 7.5% donkey serum in PBS; Molecular Probes Invitrogen) at room temperature for 3.5 h. Sections were subsequently washed 3× with PBS (10 min each), mounted with coverslips and Fluoromont-G (Southern Biotech) and sealed with clear enamel.

Fluorescence imaging was conducted with an Olympus IX71 fluorescence microscope, and images were captured using an Olympus DP70 camera and accompanying software. Images from corresponding ANGPTL7/CDT6- and scramble-siRNA-treated sections were taken at the same exposure. Digital images were arranged with image analysis software (Photoshop CS; Adobe, Mountain View, CA, USA). Negative controls were run in parallel but were incubated in blocking buffer in place of the primary antibody. Quantification of the fluorescence intensities in treated and control images was carried out using MetaMorph for Olympus digital imaging software (Olympus). Total intensity of the area of the trabecular meshwork was measured in the red channel by tracing the region in the treated image and transfer it to the control image using the transfer region and region statistics tools of the program.

For morphology, specimens were rinsed in distilled water after fixation and transferred to 70% ethanol for delivery to the UNC Histology Core for paraffin embedding. Meridional, 5-μm sections were stained with Hematoxilin and Eosin (H&E) for light microscopy evaluation.

Acknowledgements

The authors thank the members of the laboratory Dr. Md. Zahidul Karim, Dr. Juan Carabana, M. Grazia Spiga, K. David Kennedy, and M. Smith for critical reading of the manuscript. This work was supported by the National Institutes of Health (USA) grants EY11906 (TB) and EY13126 (TB), and by a Research to Prevent Blindness unrestricted grant to the UNC Department of Ophthalmology.

References

Akarsu, A.N., Turacli, M.E., Aktan, S.G., Barsoum-Homsy, M., Chevrette, L., Sayli, B.S. & Sarfarazi, M. (1996) A second locus (GLC3B) for primary congenital glaucoma (Buphthalmos) maps to the 1p36 region. *Hum. Mol. Genet.* **5**, 1199–1203.

Armaly, M.F. & Becker, B. (1965) Intraocular pressure response to topical corticosteroids. *Fed. Proc.* **24**, 1274–1278.

Bhattacharya, S.K., Rockwood, E.J., Smith, S.D., Bonilha, V.L., Crabb, J.S., Kuchtey, R.W., Robertson, N.G., Peachey, N.S., Morton, C.C. & Crabb, J.W. (2005) Proteomics reveal Cochlin deposits associated with glaucomatous trabecular meshwork. *J. Biol. Chem.* **280**, 6080–6084.

Bill, A. & Mäepea, O. (1994) Mechanisms and routes of aqueous humor drainage. In: *Principles and Practice of Ophthalmology* (eds D.M. Albert, F.A. Jakobiec), pp. 206–226. Philadelphia: W.B. Saunders Company.

Borrás, T. (2008a) Mechanosensitive genes in the trabecular meshwork at homeostasis: elevated intraocular pressure and stretch. In: *Mechanisms of the Glaucomas: Disease Processes and Therapeutic Modalities* (eds J. Tombran-Tink, C.J. Barnstable, M.B. Shields), pp. 329–362. New York: Humana Press, Inc.

Borrás, T. (2008b) What is functional genomics teaching us about intraocular pressure regulation and glaucoma. In: *The Eye's Aqueous Humor*, 2nd Edn. (Ed M.M. Civan), pp. 323–377. San Diego: Elsevier.

Borrás, T., Rowlette, L.L., Erzurum, S.C. & Epstein, D.L. (1999) Adenoviral reporter gene transfer to the human trabecular meshwork does not alter aqueous humor outflow. Relevance for potential gene therapy of glaucoma. *Gene Ther.* **6**, 515–524.

Borrás, T., Rowlette, L.L., Tamm, E.R., Gottanka, J. & Epstein, D.L. (2002) Effects of elevated intraocular pressure on outflow facility and TIGR/MYOC expression in perfused human anterior segments. *Invest. Ophthalmol. Vis. Sci.* **43**, 33–40.

Bouis, D., Hospers, G.A., Meijer, C., Dam, W., Peek, R. & Mulder, N.H. (2003) Effects of the CDT6/ANGX gene on tumour growth in immune competent mice. *In Vivo* **17**, 157–161.

Bouis, D.R., Dam, W.A., Meijer, C., Mulder, N.H. & Hospers, G.A. (2007) Effect of CDT6 on factors of angiogenic balance in tumour cell lines. *Anticancer Res.* **27**, 2325–2329.

Bradley, J.M., Vranka, J., Colvis, C.M., Conger, D.M., Alexander, J.P., Fisk, A.S., Samples, J.R. & Acott, T.S. (1998) Effect of matrix metalloproteinases activity on outflow in perfused human organ culture. *Invest. Ophthalmol. Vis. Sci.* **39**, 2649–2658.

Cadigan, K.M. (2008) Wnt-beta-catenin signaling. *Curr. Biol.* **18**, R943–R947.

Camenisch, G., Pisabarro, M.T., Sherman, D., Kowalski, J., Nagel, M., Hass, P., Xie, M.H., Gurney, A., Bodary, S., Liang, X.H., Clark, K., Beresini, M., Ferrara, N. & Gerber, H.P. (2002) ANGPTL3 stimulates endothelial cell adhesion and migration via integrin alpha vbeta 3 and induces blood vessel formation *in vivo*. *J. Biol. Chem.* **277**, 17281–17290.

Comes, N. & Borrás, T. (2007) Functional delivery of synthetic naked siRNA to the human trabecular meshwork in perfused organ cultures. *Mol. Vis.* **13**, 1363–1374.

Comes, N. & Borrás, T. (2009) Individual molecular response to elevated intraocular pressure in perfused postmortem human eyes. *Physiol. Genomics* **38**, 205–225.

Dallas, S.L., Chen, Q. & Sivakumar, P. (2006) Dynamics of assembly and reorganization of extracellular matrix proteins. *Curr. Top. Dev. Biol.* **75**, 1–24.

Faralli, J.A., Schwinn, M.K., Gonzalez, J.M. Jr, Filla, M.S. & Peters, D.M. (2009) Functional properties of fibronectin in the trabecular meshwork. *Exp. Eye Res.* **88**, 689–693.

Gerometta, R., Spiga, M.G., Borrás, T. & Candia, O.A. (2010) Treatment of sheep steroid-induced ocular hypertensionwith a glucocorticoid-inducible MMP1 Gene therapy virus. *Invest Ophthalmol. Vis. Sci.* **51**, 3042–3048.

Gonzalez, P., Epstein, D.L. & Borrás, T. (2000) Characterization of gene expression in human trabecular meshwork

using single-pass sequencing of 1060 clones. *Invest. Ophthalmol. Vis. Sci.* **41**, 3678–3693.

Hann, C.R., Springett, M.J., Wang, X. & Johnson, D.H. (2001) Ultrastructural localization of collagen IV, fibronectin, and laminin in the trabecular meshwork of normal and glaucomatous eyes. *Ophthalmic Res.* **33**, 314–324.

Hato, T., Tabata, M. & Oike, Y. (2008) The role of angiopoietin-like proteins in angiogenesis and metabolism. *Trends Cardiovasc. Med.* **18**, 6–14.

Hinz, B., Rosch, S., Ramer, R., Tamm, E.R. & Brune, K. (2005) Latanoprost induces matrix metalloproteinase-1 expression in human nonpigmented ciliary epithelial cells through a cyclooxygenase-2-dependent mechanism. *FASEB J.* **19**, 1929–1931.

Katoh, Y. & Katoh, M. (2006) Comparative integromics on Angiopoietin family members. *Int. J. Mol. Med.* **17**, 1145–1149.

Keller, K.E., Kelley, M.J. & Acott, T.S. (2007) Extracellular matrix gene alternative splicing by trabecular meshwork cells in response to mechanical stretching. *Invest. Ophthalmol. Vis. Sci.* **48**, 1164–1172.

Kim, I., Kim, H.G., Kim, H., Kim, H.H., Park, S.K., Uhm, C.S., Lee, Z.H. & Koh, G.Y. (2000) Hepatic expression, synthesis and secretion of a novel fibrinogen/angiopoietin-related protein that prevents endothelial-cell apoptosis. *Biochem. J.* **346** (Pt 3): 603–610.

Kim, I., Moon, S.O., Koh, K.N., Kim, H., Uhm, C.S., Kwak, H.J., Kim, N.G. & Koh, G.Y. (1999) Molecular cloning, expression, and characterization of angiopoietin-related protein. angiopoietin-related protein induces endothelial cell sprouting. *J. Biol. Chem.* **274**, 26523–26528.

Kitazawa, Y. & Horie, T. (1981) The prognosis of corticosteroid-responsive individuals. *Arch. Ophthalmol.* **99**, 819–823.

Knepper, P.A., Fadel, J.R., Miller, A.M., Goossens, W., Choi, J., Nolan, M.J. & Whitmer, S. (2005) Reconstitution of trabecular meshwork GAGs: influence of hyaluronic acid and chondroitin sulfate on flow rates. *J. Glaucoma* **14**, 230–238.

Knepper, P.A., Goossens, W. & Palmberg, P.F. (1996) Glycosaminoglycan stratification of the juxtacanalicular tissue in normal and primary open-angle glaucoma. *Invest. Ophthalmol. Vis. Sci.* **37**, 2414–2425.

Kuchtey, J., Kallberg, M.E., Gelatt, K.N., Rinkoski, T., Komaromy, A.M. & Kuchtey, R.W. (2008) Angiopoietin-like 7 secretion is induced by glaucoma stimuli and its concentration is elevated in glaucomatous aqueous humor. *Invest. Ophthalmol. Vis. Sci.* **49**, 3438–3448.

Lo, W.R., Rowlette, L.L., Caballero, M., Yang, P., Hernandez, M.R. & Borrás, T. (2003) Tissue differential microarray analysis of dexamethasone induction reveals potential mechanisms of steroid glaucoma. *Invest. Ophthalmol. Vis. Sci.* **44**, 473–485.

Mao, Y. & Schwarzbauer, J.E. (2005) Fibronectin fibrillogenesis, a cell-mediated matrix assembly process. *Matrix Biol.* **24**, 389–399.

Nehme, A., Lobenhofer, E.K., Stamer, W.D. & Edelman, J.L. (2009) Glucocorticoids with different chemical structures but similar glucocorticoid receptor potency regulate subsets of common and unique genes in human trabecular meshwork cells. *BMC. Med. Genomics* **2**, 58.

Oike, Y., Akao, M., Yasunaga, K., *et al.* (2005) Angiopoietin-related growth factor antagonizes obesity and insulin resistance. *Nat. Med.* **11**, 400–408.

Oike, Y., Ito, Y., Maekawa, H., Morisada, T., Kubota, Y., Akao, M., Urano, T., Yasunaga, K. & Suda, T. (2004) Angiopoietin-related growth factor (AGF) promotes angiogenesis. *Blood* **103**, 3760–3765.

Oike, Y. & Tabata, M. (2009) Angiopoietin-like proteins–potential therapeutic targets for metabolic syndrome and cardiovascular disease. *Circ. J.* **73**, 2192–2197.

Ono, M., Shimizugawa, T., Shimamura, M., Yoshida, K., Noji-Sakikawa, C., Ando, Y., Koishi, R. & Furukawa, H. (2003) Protein region important for regulation of lipid metabolism in angiopoietin-like 3 (ANGPTL3): ANGPTL3 is cleaved and activated *in vivo*. *J. Biol. Chem.* **278**, 41804–41809.

Peek, R., Kammerer, R.A., Frank, S., Otte-Holler, I. & Westphal, J.R. (2002) The angiopoietin-like factor cornea-derived transcript 6 is a putative morphogen for human cornea. *J Biol. Chem.* **277**, 686–693.

Peek, R., van Gelderen, B.E., Bruinenberg, M. & Kijlstra, A. (1998) Molecular cloning of a new angiopoietinlike factor from the human cornea. *Invest. Ophthalmol. Vis. Sci.* **39**, 1782–1788.

Quigley, H.A. (1996) Number of people with glaucoma worldwide. *Br. J. Ophthalmol.* **80**, 389–393.

Rozsa, F.W., Reed, D.M., Scott, K.M., Pawar, H., Moroi, S.E., Kijek, T.G., Krafchak, C.M., Othman, M.I., Vollrath, D., Elner, V.M. & Richards, J.E. (2006) Gene expression profile of human trabecular meshwork cells in response to long-term dexamethasone exposure. *Mol. Vis* **12**, 125–141.

Shen, X., Koga, T., Park, B.C., SundarRaj, N. & Yue, B.Y. (2008) Rho GTPase and cAMP/protein kinase A signaling mediates myocilin-induced alterations in cultured human trabecular meshwork cells. *J. Biol. Chem.* **283**, 603–612.

Tomarev, S.I., Wistow, G., Raymond, V., Dubois, S. & Malyukova, I. (2003a) Gene expression profile of the human trabecular meshwork: NEIBank sequence tag analysis. *Invest. Ophthalmol. Vis. Sci.* **44**, 2588–2596.

Tripathi, R.C., Li, J., Chan, W.F. & Tripathi, B.J. (1994) Aqueous humor in glaucomatous eyes contains an increased level of TGF-beta 2. *Exp. Eye Res.* **59**, 723–727.

Tripathi, R.C., Parapuram, S.K., Tripathi, B.J., Zhong, Y. & Chalam, K.V. (1999) Corticosteroids and glaucoma risk. *Drugs Aging* **15**, 439–450.

Vittitow, J. & Borrás, T. (2004) Genes expressed in the human trabecular meshwork during pressure-induced homeostatic response. *J. Cell. Physiol.* **201**, 126–137.

Wang, W.H., McNatt, L.G., Pang, I.H., Millar, J.C., Hellberg, P.E., Hellberg, M.H., Steely, H.T., Rubin, J.S., Fingert, J.H., Sheffield, V.C., Stone, E.M. & Clark, A.F. (2008) Increased

expression of the WNT antagonist sFRP-1 in glaucoma elevates intraocular pressure. *J. Clin. Invest.* **118**, 1056–1064.

Wight, T.N. (2002) Versican: a versatile extracellular matrix proteoglycan in cell biology. *Curr. Opin. Cell Biol.* **14**, 617–623.

Xu, A., Lam, M.C., Chan, K.W., Wang, Y., Zhang, J., Hoo, R.L., Xu, J.Y., Chen, B., Chow, W.S., Tso, A.W. & Lam, K.S. (2005) Angiopoietin-like protein 4 decreases blood glucose and improves glucose tolerance but induces hyperlipidemia and hepatic steatosis in mice. *Proc. Natl Acad. Sci. USA* **102**, 6086–6091.

Zhao, X., Ramsey, K.E., Stephan, D.A. & Russell, P. (2004) Gene and protein expression changes in human trabecular meshwork cells treated with transforming growth factor-beta. *Invest. Ophthalmol. Vis. Sci.* **45**, 4023–4034.

Received: 24 May 2010
Accepted: 16 November 2010